Novel Dynamic Scaling Regime in Hole-Doped La_2CuO_4

Wei Bao,[1] Y. Chen,[1] Y. Qiu,[2,3] and J. L. Sarrao[1]

[1]*Los Alamos National Laboratory, Los Alamos, New Mexico 87545, USA*
[2]*NIST Center for Neutron Research, National Institute of Standards and Technology, Gaithersburg, Maryland 20899, USA*
[3]*Department of Materials and Nuclear Engineering, University of Maryland, College Park, Maryland 20742, USA*

(Received 23 April 2003; published 18 September 2003)

Only 3% hole doping by Li is sufficient to suppress the long-range three-dimensional (3D) antiferromagnetic order in La_2CuO_4. The spin dynamics of such a 2D spin liquid state at $T \ll J$ was investigated with measurements of the dynamic magnetic structure factor $S(\omega, \mathbf{q})$, using cold neutron spectroscopy, for single crystalline $La_2Cu_{0.94}Li_{0.06}O_4$. $S(\omega, \mathbf{q})$ peaks sharply at (π, π) and crosses over around 50 K from ω/T scaling to a novel low temperature regime characterized by a constant-energy scale. The possible connection to a crossover from the quantum critical to the quantum disordered regime of the 2D antiferromagnetic spin liquid is discussed.

DOI: 10.1103/PhysRevLett.91.127005 PACS numbers: 74.72.Dn, 75.25.+z, 75.40.Gb, 75.50.Ee

The experimental investigation of the spin dynamics of doped Heisenberg antiferromagnets on a square lattice is essential to understanding cuprate superconductors, as well as to current research on quantum phase transitions [1]. For the structurally simplest laminar cuprate, La_2CuO_4, the three-dimensional (3D) antiferromagnetic Néel order due to weak interlayer magnetic interaction can be suppressed by 2%–3% hole doping using Sr, Ba, or Li, thus allowing experimental investigation of the quantum spin dynamics of a two-dimensional (2D) spin liquid in a wide temperature range, $0 < T \ll J/k_B \sim$ 1000 K [2].

At the critical doping concentration, y_c, of La_2CuO_4 and at $T = 0$, namely, at the quantum critical point, spin dynamics is described by classical critical dynamics in $2 + 1$ dimensions [2]. At a finite temperature, the extra dimension in imaginary time is reduced to a finite thickness of $\hbar c/k_B T$, where c is the spin wave velocity. As a consequence of this long wavelength cutoff, spin dynamics follows the quantum critical $\hbar\omega/k_B T$ scaling [3]. This has been experimentally observed in Ba and Sr doped La_2CuO_4 in previous inelastic neutron scattering studies [4–6]. At $T = 0$ and above the critical doping concentration $y > y_c$, zero-point quantum fluctuations set another long wavelength cutoff. Therefore, for $y > y_c$, when the thermal cutoff length, $\hbar c/k_B T$, reaches the quantum cutoff during cooling, a crossover in spin dynamics from the quantum critical (QC) regime, where the energy scale is $k_B T$, to the quantum disordered (QD) regime, where the energy scale is fixed at infrared by the quantum cutoff, occurs [2,3]. This crossover, however, has not been explicitly investigated experimentally. Here, we report a cold neutron inelastic scattering study on spin dynamics in Li doped La_2CuO_4 from 150 to 1.5 K. A crossover from the ω/T scaling to a new low temperature regime, which features an infrared energy cutoff, is directly observed.

The critical doping concentration, y_c, for Li doped La_2CuO_4 is 3% [7,8]. In this study, a $y = 6\%$ single crystal, $La_2Cu_{0.94}Li_{0.06}O_4$, weighing 2.1 g, was grown in CuO flux, using isotopically enriched ^{7}Li (98.4%) to reduce neutron absorption of natural Li. The crystal has orthorhombic *Cmca* symmetry with lattice parameters $a = 5.351$ Å, $b = 13.15$ Å, and $c = 5.386$ Å at 295 K. Using this orthorhombic unit cell to label reciprocal $\mathbf{q}$ space, the (π, π) point in the square lattice notation splits to (100) and (001) points. Neutron scattering signal is observed at (100)-type but not at (001)-type Bragg points, as in the stoichiometric antiferromagnet La_2CuO_4 [9]. Measurements of seven independent (100)-type Bragg peaks, using thermal neutrons to reach 6 Å^{-1}, confirm the magnetic origin of these peaks. This conclusion is consistent with previous thermal neutron scattering studies on Li doped La_2CuO_4 [10], which, however, did not have sufficient energy resolution to resolve the energy spectra at low temperatures. Here, we focus on spin dynamics near $\mathbf{q} = (100)$, taking advantage of the enhanced energy resolution of the cold neutron triple-axis spectrometer SPINS at NIST with fixed $E_f = 3.7$ or 5 meV. The (002) reflection of pyrolytic graphite was used for both the monochromator and analyzer. A cold Be or BeO filter was put before the analyzer to eliminate higher order neutrons. Horizontal Soller slits of 80′ were used before and after the sample. The temperature of the sample was regulated by a pumped He cryostat.

Figure 1 shows some constant-energy ($\hbar\omega$) scans (a) in the basal plane and (b) perpendicular to the basal plane around $\mathbf{q} = (100)$ at various energies and temperatures. The sharp peak at (π, π) in Fig. 1(a) does not show appreciable change in its width over a wide energy and temperature range, suggesting a resolution-limited in-plane peak. Flat scans in Fig. 1(b) reaffirm the two dimensionality of the spin dynamics in our sample [11]. An extensive search along the (100) and (101) directions in the basal plane yielded no incommensurate peaks, such as those found in Sr doped La_2CuO_4 [12–14]. This means that the spin liquid in $La_2Cu_{0.94}Li_{0.06}O_4$ is composed of

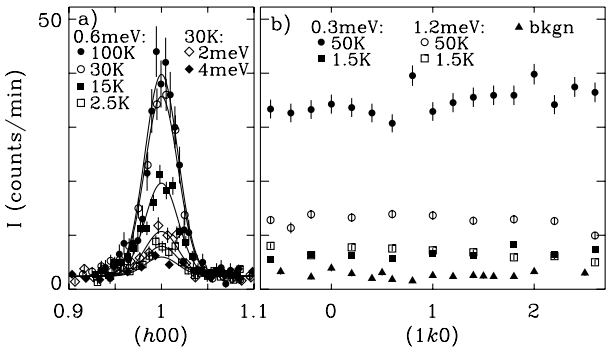

FIG. 1. Constant $\hbar\omega$ scans with various energy transfers and at various temperatures (a) in the basal CuO_2 plane and (b) perpendicular to the basal plane. The $\mathbf{q} = (100)$ here in the orthorhombic notation corresponds to the (π, π) point of the CuO_2 square plane. The background in (b), triangles, was measured at 1.5 K either at -0.5 meV or at $(1.2, k, 0)$ with $\hbar\omega = 0.3$ and 1.2 meV.

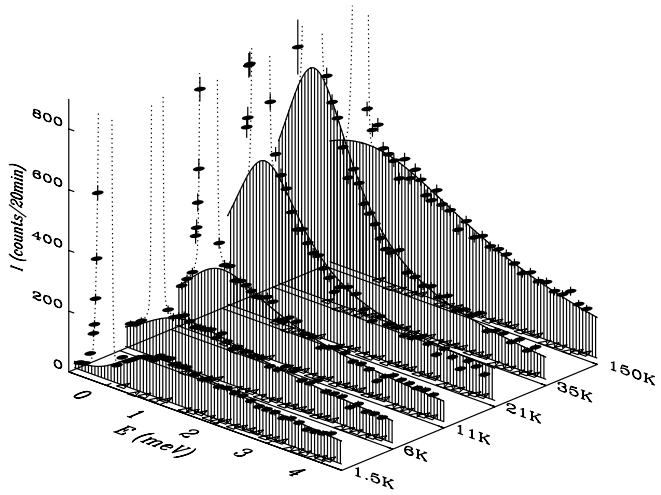

FIG. 2. Constant $\mathbf{q} = (100)$ scans from 1.5 to 150 K. The shaded area represents least-squares fit of inelastic magnetic intensity, $I(\omega)$, to Eqs. (2)–(6). Triangles represent a flat background measured at (1.39, 0, 0).

simple chessboard-type dynamic antiferromagnetic spin clusters in the CuO_2 plane, which have grown to substantial size below 100 K with the correlation length, $\xi \gg 42$ Å, the inverse of the half width at half maximum of the in-plane peak. The correlation length is much longer than the mean distance between Li dopants, 15 Å.

The commensurate spatial magnetic structure in Li doped La_2CuO_4, which is simpler than incommensurate structures observed in Sr doped La_2CuO_4 [12,14], may be understood in light of the mobility of doped holes [8,15]. Microscopic calculations have shown that the holes are loosely bound by the Li dopants [16]. Vortices associated with the holes, which are a long-range and effective topological disturbance to the 3D Néel order, preserve the commensurate (π, π) magnetic correlations [16,17]. The incommensurate magnetic structures, on the other hand, through either the "stripe" [18] or the nesting Fermi surface [19] mechanism, require more mobile holes such as those in Sr doped La_2CuO_4 [15]. The effect of hole mobility on spatial magnetic correlations has also been demonstrated in numerical simulation [20].

After delimiting the spatial part of spin dynamics in $La_2Cu_{0.94}Li_{0.06}O_4$, we now turn to the temporal dependence of the 2D (π, π)-correlated spin liquid. Figure 2 shows energy scans at $\mathbf{q} = (100) = (\pi, \pi)$ at various temperatures. Since magnetic intensity is sharply confined in $\mathbf{q}$ space in a rod passing through (100), as shown in Fig. 1, the energy scan at (1.39, 0, 0), which is far away from the rod (triangles in Fig. 2), offers a good measure of background. In addition to the flat background, neutron scattering intensity in Fig. 2 consists of a convolution of the instrument resolution function with the dynamic magnetic structure factor $S(\omega, \mathbf{q})$ plus the elastic and incoherent peak at $\omega = 0$ [21]. The imaginary part of the generalized magnetic susceptibility $\chi''(\omega, \mathbf{q})$ is related to the dynamic magnetic structure factor $S(\omega, \mathbf{q})$ by the fluctuation-dissipation theorem [22],

$$\chi''(\omega, \mathbf{q}) = \pi(1 - e^{-\hbar\omega/k_BT})S(\omega, \mathbf{q}). \quad (1)$$

The fact that there is little change in measured $\mathbf{q}$ widths in our energy and temperature ranges (Fig. 1) indicates that magnetic intensity in Fig. 2 is proportional to the *local* dynamic magnetic structure factor, $I(\omega) \propto \int d\mathbf{q} S(\omega, \mathbf{q})$. Therefore,

$$\chi''(\omega) \equiv \int d\mathbf{q}\chi''(\omega, \mathbf{q}) = C(1 - e^{-\hbar\omega/k_BT})I(\omega), \quad (2)$$

where C is a normalization constant. The commensurate spatial magnetic correlations and sharp in-plane peak (long correlation length) make measurement of the local dynamic magnetic susceptibility, $\chi''(\omega)$, in $La_2Cu_{0.94}Li_{0.06}O_4$ considerably easier than in Sr or Ba doped La_2CuO_4, which requires scans through the quartet of incommensurate satellite peaks at each ω [4–6].

$\chi''(\omega)$, obtained through Eq. (2) from scans such as those in Fig. 2, is shown as a normalized function of the dimensionless scaling variable, $\hbar\omega/k_BT$, on a semilogarithmic scale in Figs. 3(a) and 3(b). The scaling parameter χ_π is shown in Fig. 4 (diamond) as a function of temperature. ω/T scaling of $\chi''(\omega)$, which has been thoroughly investigated in pioneering works on Ba and Sr doped La_2CuO_4 [4–6], is also valid above 50 K for our Li doped sample $La_2Cu_{0.94}Li_{0.06}O_4$. In Fig. 3(a), the 150, 120, 90 and 60 K data are scaled onto a single universal curve

$$\chi''(\omega)/\chi_\pi = f(\hbar\omega/k_BT), \quad (3)$$

with the scaling function

$$f(x) = \frac{0.18x}{0.18^2 + x^2}, \quad (4)$$

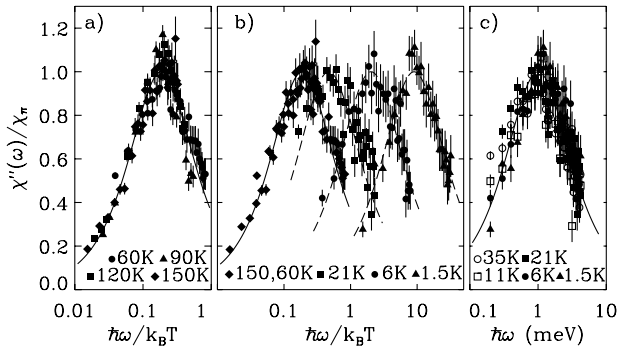

FIG. 3. (a) ω/T scaling is valid for $La_2Cu_{0.94}Li_{0.06}O_4$ in the high temperature QC regime. The solid line is the scaling function, Eq. (4). (b) ω/T scaling becomes invalid in the low temperature regime. (c) A new scaling for the low temperature regime, with a constant-energy scale $\Gamma_0 \approx 1$ meV. The solid line is the scaling function, Eq. (6).

validating the quantum critical behavior at high temperatures. The factor, 0.18, between the energy scale and thermal energy k_BT is similar to that in the insulating phase of Ba doped La_2CuO_4 [4].

Below 50 K, however, the ω/T scaling breaks down in $La_2Cu_{0.94}Li_{0.06}O_4$, as clearly shown in Fig. 3(b). Data taken at 1.5, 6, and 21 K no longer fall on the solid ω/T scaling curve, Eq. (4), valid above 50 K. Instead, a new scaling scheme describes the low temperature regime of the spin liquid. Figure 3(c) shows the normalized $\chi''(\omega)$ as a function of energy for data taken at low temperatures. All data are described by

$$\chi''(\omega)/\chi_\pi = g(\hbar\omega/\Gamma_0), \tag{5}$$

with the energy scale $\Gamma_0 \approx 1$ meV and the scaling function

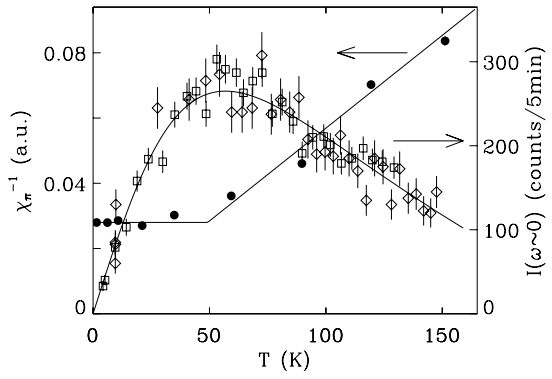

FIG. 4. Left-hand scale: Temperature dependence of inverse local magnetic susceptibility χ_π^{-1} (circles) for $La_2Cu_{0.94}Li_{0.06}O_4$; see Eqs. (3) and (5). Right-hand scale: Temperature dependence of magnetic intensity (open symbols) measured at $\hbar\omega = 0.2$ meV, $I(\omega \sim 0)$. The diamonds and squares were measured during cooling and warming, respectively.

$$g(x) = \frac{x}{1 + x^2}. \tag{6}$$

Notice also that χ_π is basically constant below 50 K (Fig. 4); therefore, $\chi''(\omega)$ is essentially independent of temperature in the new low temperature regime.

The crossover from the high temperature QC regime to the new low temperature regime also manifests itself in low-energy magnetic neutron scattering intensity. At high temperatures, from Eqs. (2)–(4),

$$I(\omega \to 0) \propto \chi_\pi \sim T^{-1}. \tag{7}$$

Therefore, magnetic intensity at the low-energy limit increases during cooling as the local magnetic susceptibility, $\chi'(0) = \pi\chi_\pi/2$, does, consistent with common paramagnetic behavior. Below the crossover temperature, from Eqs. (2), (5), and (6) and noting the constant χ_π in this regime,

$$I(\omega \to 0) \propto T, \tag{8}$$

which is markedly different from that in the QC regime, Eq. (7). Open symbols in Fig. 4 show $I(\omega)$ measured at $\mathbf{q} = (100)$ and $\hbar\omega = 0.2$ meV ~ 0, the lowest accessible energy outside the elastic incoherent peak (see Fig. 2). The $I(\omega \sim 0)$ changes from an increasing to a decreasing function of temperature as a consequence of the crossover in spin dynamics. This is consistent with Eqs. (8) and (7). The crossover temperature is around 50 K, where $I(\omega \sim 0)$ peaks and χ_π begins to saturate. The crossover temperature is also consistent with $\Gamma_0/0.18k_B$, obtained from equating the energy scales of the two regimes.

We have shown in this cold neutron inelastic study that spin dynamics in $La_2Cu_{0.94}Li_{0.06}O_4$ crosses over around 50 K from the quantum critical ω/T scaling to a new low temperature regime, characterized by a fixed energy scale and a temperature invariant spectrum $\chi''(\omega)$ in Eqs. (5) and (6). Now let us discuss the possible nature of the new regime.

In Sr or Li doped La_2CuO_4, a spin glass transition occurs in a wide doping range at a similar temperature, $T_{sf} \sim 10$ K [23–25]. In $La_2Cu_{0.94}Li_{0.06}O_4$, $T_{sf} = 8$ K [25]. This raises the possibility that the departure from the ω/T scaling at low temperature might be caused by the spin glass transition. However, the key spectral signature of a spin glass transition is a zero energy scale as the time scale becomes infinite [26]. Instead of approaching zero, the energy scale of $La_2Cu_{0.94}Li_{0.06}O_4$ saturates at a finite energy, $\Gamma \approx 1$ meV at the crossover. Therefore, the crossover around 50 K is not related to the spin glass transition.

A second possibility is to identify the low temperature regime with the quantum disordered regime of the 2D Heisenberg antiferromagnet, which is characterized by a constant-energy scale. As discussed in the introduction, the finite energy scale is determined by the quantum long wavelength cutoff, which depends on the distance from

the quantum critical point, $y - y_c$ [2,3]. Physically, the distance can be tuned by microscopic mechanisms, such as frustrating magnetic interactions [2,27], or vortexlike topological magnetic defects associated with holes [16,17]. In $La_2Cu_{0.94}Li_{0.06}O_4$, the latter mechanism may apply. Note that the finite long wavelength cutoff due to hole-induced magnetic vortices here is different from the upper cutoff length of percolating cluster on a square lattice, which is infinite for $y \lesssim 40\%$, as shown in a neutron scattering study on Zn and Mg doped La_2CuO_4 [28].

In real materials, there are additional low temperature phase transitions, which are caused by effects ignored in theoretic models of the 2D quantum antiferromagnet [2,3,27]. These transitions include (i) a finite temperature Néel transition due to weak interlayer magnetic interaction, (ii) a spin glass transition due to disorder unavoidable with doping, (iii) stripe formation [18] due to the interaction between antiferromagnetic order and mobile holes, and (iv) superconducting transition. Nevertheless, 2D quantum antiferromagnetism can be accessed in the temperature window between J/k_B and the undesired low temperature phase transitions. The QC regime [4–6] as well as the renormalized classical regime [29–32] of the 2D antiferromagnetic spin liquid have been successfully investigated experimentally in this window. Here, a possible QC to QD crossover around 50 K falls also within $J \sim 1000$ K and T_{sf}.

In effective low temperature theories based on the 2D quantum nonlinear σ model, which simulates the Néel order suppressing effect of hole doping with frustration in magnetic interactions, the scaling function $g(x)$ is usually gapped [2,27]. When interaction between spin excitations and doped fermions is explicitly considered, however, $g(x)$ becomes gapless [33,34]. The gapless $g(x)$ observed in $La_2Cu_{0.94}Li_{0.06}O_4$, Eq. (6), may be an indicator of coupling between holes and spin dynamics in doped cuprates. More recently, quantum orders are analyzed generally using projective symmetry groups [35]. Hundreds of symmetric spin liquids have been constructed, which can be grouped into four classes. Of the three stable classes in 2D, two are gapless.

In summary, the (π, π)-correlated dynamic spin clusters in hole-doped $La_2Cu_{0.94}Li_{0.06}O_4$ have developed to substantial size below 150 K. The dynamics of such spin clusters cross over around 50 K from the quantum critical ω/T scaling to a new low temperature regime with a saturated energy scale at $\Gamma_0 \approx 1$ meV. The observed crossover possibly corresponds to the theoretically expected quantum critical to quantum disordered crossover for 2D antiferromagnet.

We thank S.-H. Lee for hospitality and assistance at NIST, and P. C. Hammel, C. Broholm, A. Zheludev, L. Yu, E. Tosatti, S. Sachdev, A. V. Chubukov, F. C. Zhang, C. M. Varma, G. Aeppli, J. Haase, P. Carretta, N. J. Curro, E. Dagotto, A. V. Balatsky, Y. Bang, A. Abanov, D. Pines, R. Heffner, P. Littlewood, and A. P. Ramirez for useful discussions. SPINS at NIST is supported by NSF. Work at LANL is supported by the U.S. Department of Energy.

[1] S. Sachdev, Science **288**, 475 (2000).
[2] S. Chakravarty, B. I. Halperin, and D. R. Nelson, Phys. Rev. Lett. **60**, 1057 (1988).
[3] S. Sachdev and J. Ye, Phys. Rev. Lett. **70**, 3339 (1993).
[4] S. M. Hayden *et al.*, Phys. Rev. Lett. **66**, 821 (1991).
[5] B. Keimer *et al.*, Phys. Rev. Lett. **67**, 1930 (1991).
[6] G. Aeppli *et al.*, Science **278**, 1432 (1997).
[7] A. I. Rykov *et al.*, Physica (Amsterdam) **247C**, 327 (1995).
[8] J. L. Sarrao *et al.*, Phys. Rev. B **54**, 12014 (1996).
[9] D. Vaknin *et al.*, Phys. Rev. Lett. **58**, 2802 (1987).
[10] W. Bao *et al.*, Phys. Rev. Lett. **84**, 3978 (2000).
[11] G. Shirane *et al.*, Phys. Rev. Lett. **59**, 1613 (1987).
[12] S.-W. Cheong *et al.*, Phys. Rev. Lett. **67**, 1791 (1991).
[13] K. Yamada *et al.*, Phys. Rev. B **57**, 6165 (1998).
[14] M. Matsuda *et al.*, Phys. Rev. B **62**, 9148 (2000).
[15] H. Takagi *et al.*, Phys. Rev. Lett. **69**, 2975 (1992).
[16] S. Haas *et al.*, Phys. Rev. Lett. **77**, 3021 (1996).
[17] C. Timm and K. H. Bennemann, Phys. Rev. Lett. **84**, 4994 (2000).
[18] J. M. Tranquada *et al.*, Nature (London) **375**, 561 (1995).
[19] Q. Si *et al.*, Phys. Rev. B **47**, 9055 (1993).
[20] C. Buhler *et al.*, Phys. Rev. B **62**, R3620 (2000).
[21] Quasielastic intensity at (100) exhibits a $1/T$ dependence between 150 and 20 K, then reaches a plateau below 20 K in this neutron scattering study. Elastic signal due to spin freezing, measured with μSR, appears below 8 K [25]. These are similar to μSR and neutron scattering results of $La_{1.94}Sr_{0.06}CuO_4$; refer to B. J. Sternlieb *et al.*, Phys. Rev. B **41**, 8866 (1990).
[22] S. W. Lovesey, *Theory of Neutron Scattering from Condensed Matter* (Clarendon Press, Oxford, 1984).
[23] F. C. Chou *et al.*, Phys. Rev. Lett. **71**, 2323 (1993).
[24] C. Niedermayer *et al.*, Phys. Rev. Lett. **80**, 3843 (1998).
[25] R. H. Heffner *et al.*, Physica (Amsterdam) **312B**, 65 (2002).
[26] S. M. Shapiro, in *Spin Waves and Magnetic Excitations*, edited by A. S. Borovik-Romanov and S. K. Sinha (Elsevier, Amsterdam, 1988), Vol. 2, pp. 219–257.
[27] S. Sachdev, *Quantum Phase Transitions* (Cambridge University Press, Cambridge, 1999).
[28] O. P. Vajk *et al.*, Science **295**, 1691 (2002).
[29] R. J. Birgeneau *et al.*, Phys. Rev. B **59**, 13788 (1999).
[30] M. Greven *et al.*, Phys. Rev. Lett. **72**, 1096 (1994).
[31] H. M. Rønnow, D. F. McMorrow, and A. Harrison, Phys. Rev. Lett. **82**, 3152 (1999).
[32] P. Carretta *et al.*, Phys. Rev. Lett. **84**, 366 (2000).
[33] S. Sachdev, A. V. Chubukov, and A. Sokol, Phys. Rev. B **51**, 14874 (1995).
[34] Y. L. Liu and Z. B. Su, Phys. Lett. A **200**, 393 (1995).
[35] X. G. Wen, Phys. Rev. B **65**, 165113 (2002).